Vacancy-Vacancy Interaction on Ge-Covered Si(001)

Xun Chen, Fang Wu, Zhenyu Zhang, and M. G. Lagally
University of Wisconsin, Madison, Wisconsin 53706
(Received 28 February 1994)

When Ge atoms are deposited onto a Si(001) substrate, dimer vacancies are created in the strained system. At sufficiently high concentrations, interactions between the vacancies cause them to line up, resulting in the $(2 \times n)$ reconstruction. By analyzing the thermal fluctuations around the ideal $(2 \times n)$ structure with scanning tunneling microscopy and using transfer matrix theory, the form of the dimer vacancy-vacancy interaction and a value for its magnitude have been determined.

PACS numbers: 68.35.Md, 68.35.Bs, 68.35.Dv

In lattice-mismatched overlayer systems, the effort of the system to minimize lattice strain can produce defects such as misfit dislocations and vacancies. The interaction between these defects may lead to complicated surface reconstruction. The heteroepitaxy of Ge on Si(001) serves as a model lattice-mismatched system. Bulk Ge has a lattice constant 4.3% larger than that of Si. When Ge atoms are deposited on the Si surface, they arrange themselves in registry with the substrate Si atoms, but the Ge overlayer is compressed in order to accommodate the 4.3% difference in lattice size. The strong strain field produced in the system is responsible, at least partially, for a number of phenomena, including the increase of dimer vacancy concentration in the surface layer with increasing Ge coverage [1], the ordering of the dimer vacancies into the $(2 \times n)$ reconstruction [2–4], reversal of the relative step roughness [5,6], the formation of "microhuts" [7], and the Stranski-Krastanov growth mode for Ge films on Si [8].

On a clean Si(001) surface, the top-layer atoms dimerize and the dimers align to form dimer rows, leading to the (2×1) reconstruction [9,10]. On a Ge-covered Si(001) surface, dimer rows still form, but the surface reconstruction does not have a simple (2×1) symmetry. Instead, some dimers are missing, leaving behind dimer vacancies (DV's). With increasing Ge coverage, DV's on different dimer rows order in the direction perpendicular to the dimer rows, forming vacancy lines (VL's). On average, two adjacent VL's are separated by na_0, giving rise to the $(2 \times n)$ reconstruction; a_0 here is the surface lattice spacing. Figure 1 shows a scanning tunneling microscopy (STM) image of this $(2 \times n)$ structure, where the VL's are visible as dark lines.

The ordering of the dimer vacancies is driven by an intrinsic dimer vacancy-vacancy (DV-DV) interaction, whose form and strength have been unknown. In this Letter, we carry out an experimental and theoretical study of this interaction. The surface morphology, in particular the meandering of the VL's, is dictated by the competition between the ordering process, driven by the DV-DV interaction, and the disordering process, driven by a desire of the system to minimize its free energy.

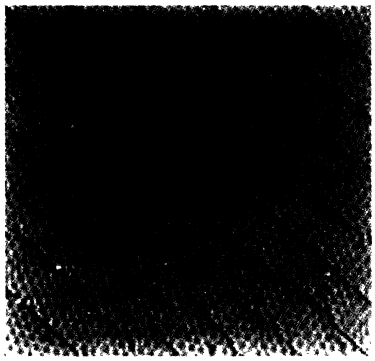

FIG. 1. STM image of the Ge-covered Si(001) surface showing the $(2 \times n)$ reconstruction. Size of the image is $\sim 350 \times 350$ Å^2. The Ge coverage is ~ 1.5 ML. The dark lines are dimer vacancy lines, which are perpendicular to the dimer rows.

By analyzing the thermal fluctuations around the ideal $(2 \times n)$ structure using STM, we determine the form as well as the magnitude of the DV-DV interaction.

The experiment is carried out in UHV. Silicon (001) samples with miscut angles less than 0.03° are used as substrates. They are cleaned by flashing to above 1200 °C and subsequently annealed at 600 °C for 5 min before Ge deposition; this procedure is known to yield atomically clean Si surfaces [11]. The deposition rate is ~ 0.01 monolayer (ML)/min from a resistively heated Ge wafer. About 1.5 ML of Ge is deposited on a Si(001) substrate held at 400 °C; the overlayer is annealed at the same temperature for 1 h to allow for the equilibration of the meandering of vacancy lines; and the sample is then quenched and transferred to the STM for imaging. The radiation quench brings the substrate temperature from 700 to 400 K in less than 10 s. Using the observation [12] that the diffusion of dimer vacancies on clean Si(001) occurs on the time scale of one displacement in ~ 15 s at 500 K, we estimate the equilibrium temperature corresponding to the vacancy line morphology we observe at room temperature to lie between 500 and 700 K. Topographic STM images are taken with a sample bias $V_s \sim -2$ V, and a tunneling current $I_t \sim 0.1$ nA.

0031-9007/94/73(6)/850(4)$06.00

The vacancy lines shown in Fig. 1 are not straight. The meandering of a VL results from thermally induced relative displacements between neighboring vacancies (see Fig. 2). By studying the statistical properties of these displacements, we can extract detailed information on the DV-DV interaction. Before going into any mathematical details, we discuss qualitative features of this interaction. It has been proposed [13] and supported by calculations [1] that, within each DV, the second-layer atoms rebond. The rebonded atoms are pulled together (see Fig. 2), giving rise to a large tensile stress *along* the top-layer dimer row. The rebonding does not induce any long-range elastic field in the *perpendicular* direction [1]. The tensile stress due to second-layer rebonding partially cancels the compressive stress due to Ge/Si lattice mismatch, thus lowering the elastic energy. There exists a preferred spacing na_0 between two neighboring DV's on the same dimer row. When they are too far apart, the compressive stress is not relieved enough; if they are too close, the stress is "over-relieved." Effectively, this balancing of tensile and compressive stresses amounts to a short-range repulsive, long-range attractive interaction between DV's on the *same* dimer row [1,14], i.e., the qualitative features of the vacancy interaction suggested by Ref. [1] should be applicable. When individual DV's are on *different* dimer rows, the interaction between them must be short-range attractive, based on the very fact that they prefer to order into vacancy lines.

The qualitative analysis given above reveals the nature of the problem we must tackle: a two-dimensional (2D) interacting system. Fortunately, to a very good approximation this complicated problem can be simplified into a one-dimensional (1D) one. In the 1D model, the system consists of a collection of vacancy lines, each moving in an effective potential, $V(h)$, representing the collective effect of all the other VL's. The validity of this mean-field approximation will later be checked by self-consistency, but here we provide an *a priori* justification. The mean-field approximation neglects any possible correlation between the meandering of neighboring vancancy lines. Correlated meandering exists if the probability of exciting a vacancy-vacancy displacement in a given VL depends on the existence or direction of the displacements in the neighboring VL's (see Fig. 2). From the STM images, we have analyzed the probability of forming a thermal displacement in a given vacancy line, and found that it is independent of the configuration of the neighboring VL's. Therefore, the above described correlation is statistically negligible in the present case, suggesting that a mean-field approach is appropriate.

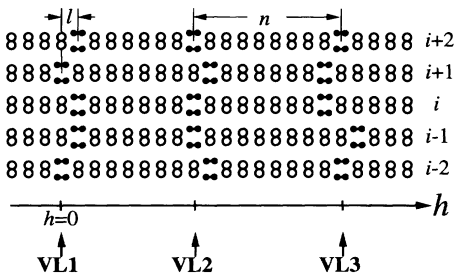

FIG. 2. A schematic diagram showing the atomic structure of the $(2 \times n)$ reconstruction. The open and solid circles represent the top- and second-layer atoms, respectively. Two connected atoms form a dimer, and the dimers align into dimer rows labeled by i, $i \pm 1$, etc. Within each dimer vacancy are four rebonded second-layer atoms. Three vacancy lines, running vertically in the picture, are labeled as VL1 to VL3. Also defined are the h axis; the distance between two neighboring vacancy lines, n; and the separation l of two vacancies on adjacent dimer rows.

The problem now reduces to understanding the behavior of a single vacancy line in an external field $V(h)$. The position of each dimer vacancy in this line is specified by h_i, with the h axis pointing in the dimer row direction, measured from the mean position of the VL. The subscript i denotes the location of the dimer row containing the vacancy (see Fig. 2). Thermal excitation causes a relative displacement between the vacancies on adjacent dimer rows, e.g., rows i and $i + 1$, making $h_i \neq h_{i+1}$, and a length of the displacement (i.e., the separation of the DV's when they are on adjacent dimer rows), $l = |h_i - h_{i+1}|$. The problem can be further simplified if the DV-DV interaction along the dimer vacancy line is very short range. Consider three consecutive dimer vacancies in a vacancy line, DV1, DV2, and DV3 (i.e., on dimer rows $i = 1, 2, 3$), and two possible relative displacements: one between DV1 and DV2 and the other between DV2 and DV3. It is straightforward to show that if there is no directional correlation between the two relative displacements, there will be no interaction between the two next-nearest-neighboring dimer vacancies (i.e., DV1 and DV3). We have measured the formation probability of a relative displacement in a VL and found that it is independent of the existence or the direction of any other relative displacement on the same vacancy line. Therefore, we can neglect any but nearest-neighbor interactions along a line of DV's. Under these constraints this problem can be solved exactly within the framework of transfer matrix theory. The Hamiltonian of the VL is

$$H[\{h_i\}] = \sum_i E(h_i, h_{i+1}) + \sum_i V(h_i), \qquad (1)$$

where each pair of adjacent DV's has an interaction energy $E(h_i, h_{i+1})$ that depends only on their separation l: $E(h_i, h_{i+1}) = E(l)$. In order to determine both $E(h_i, h_{i+1})$ and $V(h)$, we first introduce the transfer matrix, $\mathbf{T}$, whose elements are given by

$$T_{h_1,h_2} = \exp\{-\beta E(h_1, h_2) - \tfrac{1}{2}\beta[V(h_1) + V(h_2)]\}, \qquad (2)$$

where $\beta^{-1} = k_B T$, k_B is the Boltzmann constant, and T is the equilibrium temperature. Using Eqs. (1) and

(2), we can express the probability of finding a relative displacement l as

$$P(l) = \frac{2}{Z}\sum_{\{h_i\}} \delta(h_1 - h_2 - l)T_{h_1h_2}T_{h_2h_3}\cdots T_{h_{N-1}h_N}T_{h_Nh_1}, \tag{3}$$

where Z is the partition function. After some algebra, we derive from Eq. (3)

$$P(l) = \lambda_m^{-1}\exp[-\beta E(l)]\sum_{h_1}\exp\{-\tfrac{1}{2}\beta[V(h_1) + V(h_1 - l)]\} \times \sqrt{P_h(h_1)P_h(h_1 - l)}, \tag{4}$$

where λ_m is the largest eigenvalue of the transfer matrix, P_h is the distribution function of the displacements of the VL around its mean position, given by the frequency of occurrence of the DV's having a particular value of h. That is, P_h is the normalized histogram of the h coordinates of all the DV's in a VL measured from its mean position.

Because our STM images are typically about 400 Å $\times$ 400 Å, it is impossible to locate accurately the mean position of a VL solely from these images and therefore the P_h distribution cannot be obtained directly from the images. However, it can be obtained indirectly from P_n, the probability distribution of n, where n by definition is the distance between adjacent dimer vacancies on a given dimer row. In the present case, where the meandering of neighboring VL's is uncorrelated, P_n is simply a convolution of two independent probability distributions: $P_h(h_{1,i})$ and $P_h(h_{2,i})$, where $h_{1,i}$ and $h_{2,i}$ are respectively the h coordinates of two neighboring dimer vacancies on dimer row i. Therefore, once the P_n distribution is measured from the images, we can obtain P_h by deconvolution. The P_n distribution obtained by analyzing the STM images is plotted in Fig. 3 together with a Gaussian fit. The width of the Gaussian is $w_n = 1.67a_0$.

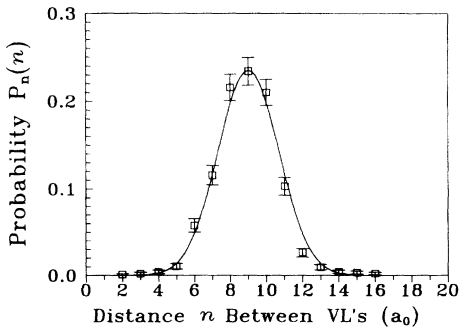

FIG. 3. The probability distribution of the separation of two neighboring dimer vacancies on the same dimer row, $P_n(n)$. More than 1000 separations are measured. The squares are experimental data and the curve is a Gaussian fit. Error bars represent statistical errors in the counting.

The deconvolution yields a Gaussian form also for P_h, but with a smaller width, $w_h = w_n/\sqrt{2} = 1.20a_0$.

The fact that the P_h distribution is Gaussian is not at all surprising if one realizes that the profile of a VL can be equivalently viewed as the trace of a 1D random walk in an external potential $V(h)$. If the potential is quadratic, $\beta V(h) = (1/2)kh^2$, the trace follows precisely a Gaussian distribution [15,16]. In the present case, our early qualitative analysis has led to the conclusion that the mean-field potential $V(h)$ has a minimum at the mean position of the VL located at $h = 0$. The leading term in the expansion of $V(h)$ at the minimum is therefore quadratic. Assuming a quadratic form for $V(h)$, and inserting into Eq. (4) together with the Gaussian form of P_h, Eq. (5), we obtain

$$\beta E(l) = -\ln\frac{P(l)}{2P(0)} - \frac{1}{8}(k + w_h^{-2})l^2. \tag{5}$$

Equation (5) provides one of the key relationships from which the interaction energy $E(l)$ between two DV's on neighboring dimer rows as a function of their separation l can be extracted. Equation (5), without the second term on the right-hand side, is the expression for the interaction energy in the case of no external confining potential $V(h)$ acting on the VL. The effect of the confinement is represented by the second term, which vanishes identically when $k = 0$ ($w_h \to \infty$ for a free random walker). In this equation, w_h has already been obtained and $P(l)$ is directly obtained from the STM images by counting the occurrence of relative displacements of length l, but the strength of the mean-field potential, k, is yet to be determined. In order to extract the values of both $E(l)$ and k simultaneously we must invoke a second relationship. This second relationship is provided by self-consistency in the Metropolis Monte Carlo simulations to generate the equilibrium configurations of the VL's using the Hamiltonian defined in Eq. (1), with the second term on the right-hand side given by $\beta V(h) = (1/2)kh^2$. For each trial value of k, $E(l)$ is calculated according to Eq. (5). The program generates equilibrium vacancy line configurations, from which the distribution $P_h(h)$ is calculated. This distribution in turn is compared to the Gaussian form with $w_h = 1.20a_0$. The trial value of k is then adjusted according to this comparison until the computer generated $P_h(h)$ converges to the correct Gaussian distribution. This convergence serves as the second relationship necessary to determine the values of $E(l)$ and k. Convergence is mandatory if the mean-field model is valid.

Our simulations following this scheme yield $k = (0.075 \pm 0.008)a_0^{-2}$. The corresponding interaction energy $E(l)$ between two dimer vacancies on adjacent dimer rows separated by l is plotted versus l in Fig. 4. This interaction is attractive and short ranged; it becomes zero when the relative displacement between the DV's on neighboring dimer rows is beyond $4a_0$. The origin

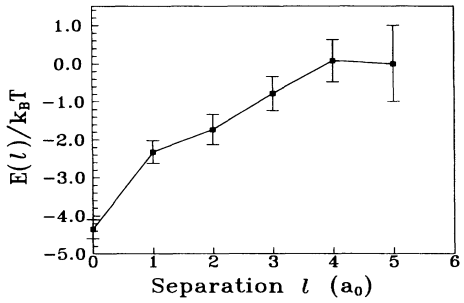

FIG. 4. The interaction energy of dimer vacancies on adjacent dimer rows vs their separation. The solid line guides the eye. The error bars contain statistical error in the counting, the error in determining w_h, and the error in the k value determined from the simulation.

of the energy axis in Fig. 4 is chosen so that $E(5) = 0$, indicating that we are using the energy of two well separated, hence noninteracting, dimer vacancies as the energy reference. If we use limits of 500 and 700 K for the temperature at which the VL's in Fig. 1 are at equilibrium, the strength of the attractive interaction, or equivalently the binding energy of two dimer vacancies, is between 180 and 250 meV. The physical origin of this attractive interaction is probably a delicate relaxation of the local atomic structure around the two neighboring dimer vacancies. When a vacancy is created on the surface, atoms around it relax to find the lowest energy configuration. For two close-lying vacancies, the local relaxation associated with each vacancy will overlap and interfere, leading to an effective interaction between the vacancies. Preliminary results of calculation of vacancy interaction energies in Si(001) using a Stillinger-Weber potential and allowing complete relaxation of the surrounding atoms confirm the form, the range, and the order of magnitude of this interaction [14].

Because of the likely intermixing of Ge and Si [17], the main results here are obtained for an unknown stoichiometry of the topmost layers. The determination of this stoichiometry is extremely difficult and cannot be done by STM. The exact value of the interaction energy and the strain field associated with each dimer vacancy are expected to depend on the composition of the topmost layers. The interaction energies are also expected to depend on the Ge coverage. At higher coverage of Ge, for example, 3 ML as in Ref. [1], the overlayer starts to break into islands. We chose 1.5 ML of Ge for our analysis to avoid the additional complexities introduced by the islands.

In conclusion, the dimer vacancies on a Ge-covered Si(001) surface interact strongly with each other, and the interaction is highly anisotropic. For dimer vacancies on the same dimer row, the interaction is short-range repulsive and long-range attractive and balances at na_0. The interaction can be well described by a mean-field potential, a manifestation of the elastic field associated with the dimer vacancies. On the other hand, a short-range attractive interaction exists between dimer vacancies on different dimer rows. It is significant only when the dimer vacancies are on adjacent dimer rows. The interaction energy between these dimer vacancies is determined as a function of their separation. The binding energy (i.e., at zero separation) is on the order of 200 meV and falls off to zero in about four lattice constants. The physical origin of this interaction is likely the local structural relaxation associated with each vacancy.

This work was supported by NSF, Solid State Chemistry Program, Grant No. DMR93-04912 and ONR, Physics Program.

[1] J. Tersoff, Phys. Rev. B **45**, 8833 (1992).
[2] Y.-W. Mo and M. G. Lagally, J. Cryst. Growth **111**, 876 (1991).
[3] U. Köhler, O. Jusko, B. Müller, M. Horn-von Hoegen, and M. Pook, Ultramicroscopy **42–44**, 832 (1992).
[4] R. Butz and S. Kampers, Appl. Phys. Lett. **61**, 1307 (1992).
[5] F. Wu, X. Chen, Z. Y. Zhang, and M. G. Lagally (to be published).
[6] E. Umbach and J. Blakely (to be published).
[7] Y.-W. Mo, D. E. Savage, B. S. Swartzentruber, and M. G. Lagally, Phys. Rev. Lett. **65**, 1020 (1990).
[8] D. J. Eaglesham and M. Cerullo, Phys. Rev. Lett. **64**, 1943 (1990).
[9] R. Schlier and H. Farnsworth, J. Chem. Phys. **30**, 917 (1959).
[10] R. M. Tromp, R. J. Hamers, and J. E. Demuth, Phys. Rev. Lett. **55**, 1303 (1985).
[11] B. S. Swartzentruber, Y.-W. Mo, M. B. Webb, and M. G. Lagally, J. Vac. Sci. Technol. A **7**, 2901 (1989).
[12] N. Kitamura, M. G. Lagally, and M. B. Webb, Phys. Rev. Lett. **71**, 2082 (1993).
[13] K. C. Pandey, in *Proceedings of the International Conference on the Physics of Semiconductors*, edited by D. J. Chadi and W. A. Harrison (Springer, Berlin, 1985), p. 55.
[14] P. Weakliem, Z. Y. Zhang, X. Chen, F. Wu, H. Metiu, and M. G. Lagally (to be published).
[15] M. E. Fisher and D. S. Fisher, Phys. Rev. B **25**, 3192 (1982).
[16] N. C. Bartelt, T. L. Einstein, and E. D. Williams, Surf. Sci. Lett. **240**, L791 (1990).
[17] R. Tromp, Phys. Rev. B **47**, 7125 (1993).

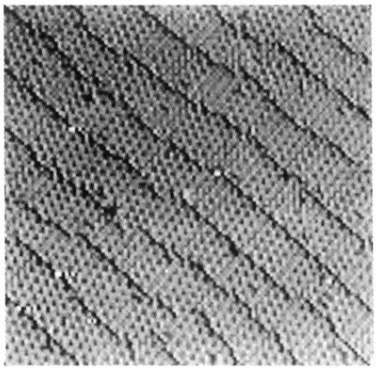

FIG. 1. STM image of the Ge-covered Si(001) surface showing the $(2 \times n)$ reconstruction. Size of the image is $\sim 350 \times 350$ Å^2. The Ge coverage is ~ 1.5 ML. The dark lines are dimer vacancy lines, which are perpendicular to the dimer rows.